Chapter 7 The Quantum Hall effect

In many cases, transport in higer dimensions can be understood as that in networks of one-dimensional quantum wires. On the other hand in the case of Landau quantization, mixing of two-dimensional freedoms is important and it is easier to treat the system as continuous two-dimensional space (see Sec.[**?**] for discrete treatment)..

10.1 Two-dimensional electrons under magnetic field

Let us write the Hamiltonian as

$$\mathscr{H} = \frac{m}{2}\boldsymbol{v}^2 = \frac{(\boldsymbol{p}_c + e\boldsymbol{A})^2}{2m} \equiv \frac{\boldsymbol{\pi}^2}{2m} = \frac{\pi_x^2 + \pi_y^2}{2m}. \tag{10.1}$$

$$\boldsymbol{\pi} \equiv \boldsymbol{p}_c + e\boldsymbol{A}, \tag{10.2}$$

where $\boldsymbol{\pi}$ is dynamical momentum, corresponding to real space velocity as $\boldsymbol{v} = \boldsymbol{\pi}/m^*$. $\boldsymbol{\pi}$ has commutation relations among themselves and with space coordinates as

$$[\pi_\alpha, \beta] = -i\hbar\delta_{\alpha\beta}, \quad (\alpha, \beta = x, y), \quad [\pi_x, \pi_y] = -i\frac{\hbar^2}{l^2}. \tag{10.3}$$

We see that x and y components of the momentum do not commute. The fact corresponds to the classical circulating orbits, which mix up the x and y coordinates, in other words they are no longer independent. l is called **magnetic length** defined as

$$l \equiv \sqrt{\frac{\hbar}{eB}} = \sqrt{\frac{1}{2}}\sqrt{\frac{\phi_0}{\pi B}}, \tag{10.4}$$

which is $1/\sqrt{2}$ times the radius of circle for single flux quantum ($\phi_0 \equiv h/e$). l is also called minimum Landau radius. The factor $1/\sqrt{2}$ corresponds to the zero-point energy term $\hbar\omega_c/2$ in Eq. (10.9), which we will see later.

We define the operator $\hat{\boldsymbol{R}}$ of guiding center coordinate (X, Y) as

$$\hat{\boldsymbol{r}} = \hat{\boldsymbol{R}} + \frac{l^2}{\hbar}(\pi_y, -\pi_x), \tag{10.5}$$

where $\hat{\boldsymbol{r}}$ is the real space operator of electrons. The second term in the right hand side is from the classical solution (not in this note). From the commutation relation between π_x and π_y, we get

$$[X, Y] = il^2. \tag{10.6}$$

The Hamiltonian does not depend on (X, Y), thus (X, Y) is a constant of motion while from the commutation relation in (10.6), there is an uncertainty between X and Y. Now we see that as a set of canonically conjugate variables of the system we can take $\boldsymbol{R}$, $\boldsymbol{\pi}$ other than $(\boldsymbol{r}, \boldsymbol{p}_c)$.

10.1.1 Landau quantization

As in (10.1), the Hamiltonian is quadratic for $\boldsymbol{\pi}$ and in the form of harmonic oscillator [*1], by introducing down/up operators as

$$a = \frac{l}{\sqrt{2}\hbar}(\pi_x - i\pi_y), \quad a^\dagger = \frac{l}{\sqrt{2}\hbar}(\pi_x + i\pi_y), \tag{10.7}$$

it can be written as

$$[a, a^\dagger] = 1, \quad \mathscr{H} = \hbar\omega_c \left(a^\dagger a + \frac{1}{2}\right). \tag{10.8}$$

This is in the harmonic form and the engenenergies are given as

$$E_n = \hbar\omega_c \left(n + \frac{1}{2}\right) \quad (n = 0, 1, 2, \cdots). \tag{10.9}$$

This is interpreted as the discretization of (angular) momentum with quantum confinement by magnetic field. Such quantization of orbitals by magnetic field is called **Landau quantization**.

10.1.2 Guiding center

Because $\boldsymbol{R}$ commutes with Hamiltonian (10.1), the eigenenergies in Eq. (10.9) do not depend on $\boldsymbol{R}$, thus they are degenerate as the degree of freedom in $\boldsymbol{R}$. Two dimensional systems under perpendicular uniform magnetic field still keeps spatial translational symmetry. In the set of eigenfunctions which have the guiding center as an index, the translational symmetry is kept through the freedom in $\boldsymbol{R}$. The Landau levels have large degeneracy and the basis can be taken in various form. The uncommutability between the components of $\boldsymbol{R}$ brings large variaty in the outlooks of the basis.

Let us find the basis that diagonalizes X. For that Landau gauge $\boldsymbol{A} = (0, Bx, 0)$ is convenient. Form Eq. (10.1), Schrödinger equation is given by

$$\begin{aligned}\mathscr{H}\psi = \frac{(\boldsymbol{p}_c + e\boldsymbol{A})^2}{2m}\psi &= \frac{-1}{2m}\left[\frac{\hbar^2\partial^2}{\partial x^2} - \left(-i\frac{\hbar\partial}{\partial y} + eBx\right)^2\right]\psi(\boldsymbol{r}) \\ &= \frac{1}{2m}\left[-\hbar^2\nabla^2 - 2i\hbar eBx\frac{\partial}{\partial y} + e^2B^2x^2\right]\psi(\boldsymbol{r}) = E\psi(\boldsymbol{r}).\end{aligned} \tag{10.10}$$

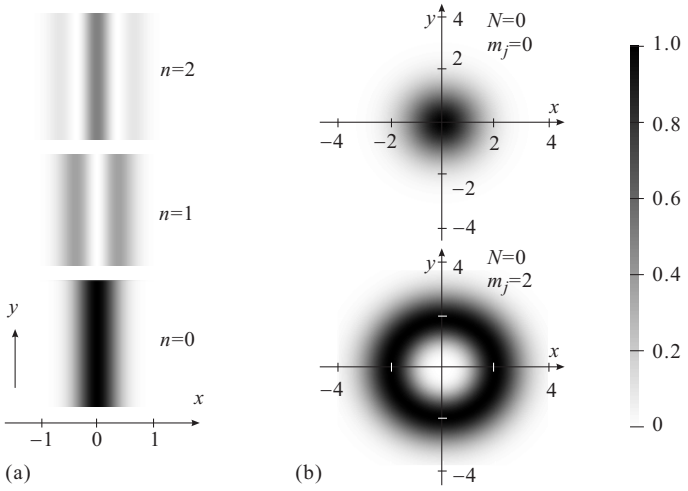

Fig. 10.1 (a) Gray scale plots of probability densities $|\psi_{n\boldsymbol{k}}(\boldsymbol{r})|^2$ in eigenstates (10.12) with three values of n, which diagonalize X. The unit of length is l_B, the width along x is about $\sqrt{2n+1}l_B$. (b) The same for the basis, which diagonalizes $X^2 + Y^2$ (not mentioned in the text). In the case of $N = 0$, the distribution is around the circle with the radius $|\sqrt{2|m_j|}l_B$ at the origin.

[*1] It is written as a sum of π_x^2 and π_y^2. π_x and π_y are canonically conjugate operators.

This Hamiltonian does not contain operator y and y-dependent part of the wavefunction should be a plane wave. Thus we substitute variable separable form $\psi(\boldsymbol{r}) = u(x)\exp(iky)$ into the above equation to obtain

$$\left[-\frac{\hbar^2}{2m}\frac{d^2}{dx^2} + \frac{(eB)^2}{2m}\left(x + \frac{\hbar}{eB}k\right)^2\right]u(x) = \left[-\frac{\hbar^2}{2m}\frac{d^2}{dx^2} + \frac{m\omega_{\rm c}^2}{2}(x + l^2k)^2\right]u(x) = Eu(x). \tag{10.11}$$

This is an equation of a one-dimensional harmonic oscillator that has the center at $x = -l^2k$. The eigenvalues are given in Eq. (10.9), and the eigenfunctions are written as

$$\psi_{nk}(\boldsymbol{r}) \propto H_n\left(\frac{x - x_k}{l}\right)\exp\left(-\frac{(x - x_k)^2}{2l^2}\right)\exp(iky) \quad (x_k \equiv -l^2k), \tag{10.12}$$

where H_n is n-th order Hermite polynomial. In each of these states, X is fixed as $X = x_k = -l^2k = -l^2p_y/\hbar$ while it is a plane wave on y spreading over whole space, namely Y is fully uncertain. In the states given by Eq. (10.12), the energy does not depend on k. Though the states are extended along y, hence the group velocity is zero ($\partial E/\partial k = 0$). On the other hand $\partial X/\partial k$ is not zero, then if some x-dependent potential is added to the system, the states gain a finite group velocity and motions along y.

Figure 10.1(a) shows gray scale plots of probability density in Eq. (10.12). We see they are uniform along y while one-dimensional harmonic oscillators along x. We are not showing the functional form here but the eigenstates can be chosen so as to diagonalize $X^2 + Y^2$. In this case, as shown in Fig. 10.1(b), the probability densities are localized both for x and y. The reason why their outlooks are so different in spite of the fact that they have the same eigenenergy, is of course it has large degeneracy and also the degeneracy comes from the freedom in $\boldsymbol{R}$, which is the freedom in the real space.

10.2 Integer quantum Hall effect

10.2.1 Shubnikov de Haas (SdH) oscillation

Let us consider the process of increasing magnetic field applied perpendicular to a two-dimensional electron system. With Landau quantization (10.9), the energy levels are as in Fig. 10.2, spead radially from the origin (Landau fan, fan diagram). How the electrons occupy those Landau levels when the system is connected to particle reservoirs as in transport experiments? The external particle reserviors make the Fermi level $E_{\rm F}$ constant but if we impose this condition, the origin in Fig. 10.2 should shift with magnetic field. The origin in Fig. 10.2 is defined as the zero-point of kinetic energy in xy-plane, namely energy levels quantized along z-axis. In the simple approximation in Sec. 7.3, the position of $E_{\rm F}$ is determined to screen the electrostatic potential formed by ionized potential with arial density $N_{\rm dep}$. Then with variation in the density of states for kinetic freedom in xy plane, the distribution of occupied states also varies to compensate the potential from the impurities. This leads to the shifts in self-consistent potential and the position of the lowest level (origin). If we look the Landau fan from the coordinate in which the origin is fixed, $E_{\rm F}$ varies with magnetic field. Below, we adopt this coordinate (constant 2DEG arial density n_s).

Let us find the arial density of states per single Ladau level $n_{\rm L}$. For that we count the number of possible wavefunctions in Eq. (10.12) in the area of $W_x \times W_y$ in xy-plane. The function in Eq. (10.12) is a plane wave along y and the "distance" of the states in k-space in $2\pi/W_y$. On the other hand, the section $0 \le X \le W_x$ corresponds to $-W_x/l_B^2 \le k \le 0$ in k-space for the wavefunctions. Hence the number of of states in the area $S = W_xW_y$ is

$$\frac{W_x/l_B^2}{2\pi/W_y} = \frac{S}{2\pi l_B^2} \quad \therefore n_{\rm L} = \frac{1}{2\pi l_B^2} = \frac{eB}{h} = \frac{B}{\phi_0}, \tag{10.13}$$

that is the number of quantum flux in the flux density. The number of Landau levels occupied by electrons is

$$\nu = \frac{\phi_0 n_s}{B}, \tag{10.14}$$

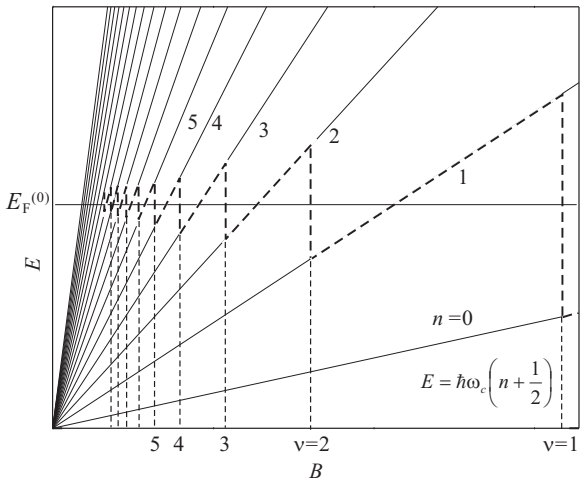

Fig. 10.2 Landau levels in (10.9) as a function of magnetic field. The broken line indicates the potision of $E_{\rm F}$ in this frame under the condition of constant n_s. $E_{\rm F}^{(0)}$ is for zero magnetic field.

which is called **filling factor**

At absolute zero, electrons occupy Landau levels from the lowest one and $E_{\rm F}$ is locked to the highest occupied Landau level. With increasing magnetic field, the changes of "topmost occupied level" take place at the points ν hit integers, where $E_{\rm F}$ shifts from $E = \hbar\omega_c(\nu + 1/2)$ to $\hbar\omega_c(\nu - 1/2)$. To summarize, in Fig. 10.2, $E_{\rm F}$ oscillates as indicated by broken line. This oscillation and the resultant oscillation in the electric resistance is called **Shubnikov-de Haas** (SdH) oscillation.

10.2.2 Localization of wavefuntion

I believe there is no rigorous proof but it is widely believed that in two-dimensional systems with some potential disorder, time-reversal symmetry, no spin-orbit interaction, all the particle states (wavefunctions) localize spatially (Anderson localization). Magnetic field breaks the time reversal smmetry and the Anderson localization is simultaneously broken. However, with further increase in magnetic field, the cyclotron radius becomes shorter than the characteristic length of the potential disorder, localization appears due to a bit different mechanism.

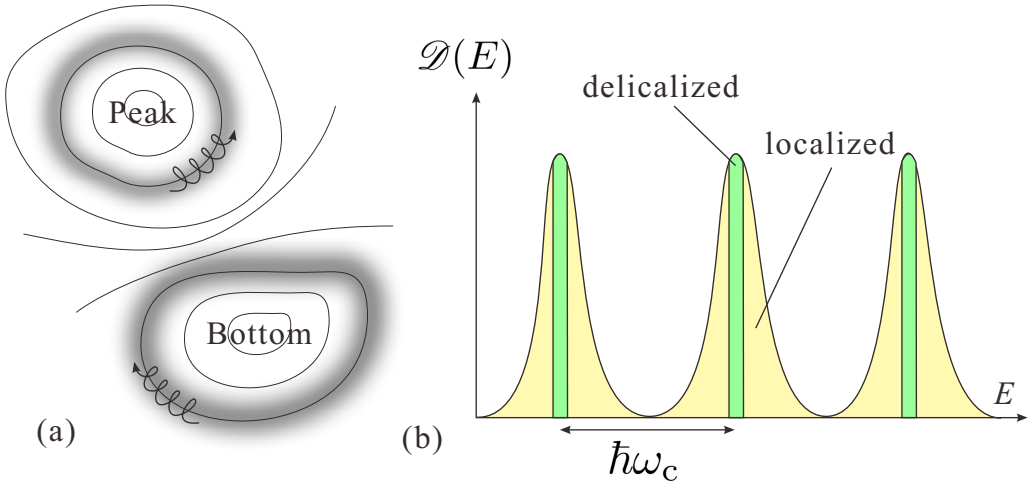

Fig. 10.3 (a) Schematic diagram showing how the Landau level wavefunction is localized by the impurity potential in a strong magnetic field. Wavefunctions in the form of Fig. 10.1(a) are bound on equipotential lines of disordered potential. The lines that depict drifting while rotating are classical orbits. (b) Landau level energies are broadened by disordered potential and localized as shadowed. Delocalized states exist around the centers of Landau "bands," corresponding to the concave-convex transition equipotential lines.

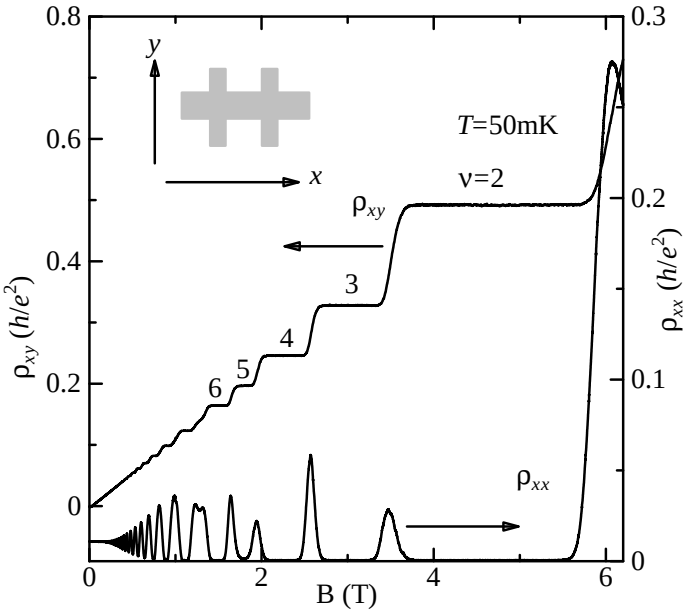

Fig. 10.4 Example of integer quantum Hall effect. 2DEG at an AlGaAs/GaAs interface is fabricated into the shape of Hall bar shown in the inset. A current is applied to the long thick line (x-direction), ρ_{xx} is obtained from the voltage between two probes placed along x while ρ_{xy} is obtained from the probes placed face to face along y.

Such behavior is illustrated in Fig. 10.3(a). Electric field applied to electons in cyclotron motion causes movement perpenducular to the field. In nonuniform potential as shown in the figure, such movement of electrons results in a rounding motion bound on an equipotential line. Then the state as a whole is spatially localized. Such spatial confinement leads to broadening of Landau levels as we have seen in Fock-Darwin state. Then the delta-function density of states of original Ladau level gets broadening as illustrated in Fig. 10.3(b). On the other hand, there are a small number of equipotential lines that do not make a closed loop between potential peaks and dips as in Fig. 10.3(a). Such a state on non-closed equipotential line should be extended and it is known that each broadened Landau "band" has a single such extended state at the center. This is also illustrated in Fig. 10.3(b).

10.2.3 Characteristics of integer quantum Hall effect

In Fig. 10.4 we show an example of measured integer quantum Hall effect (IQHE). Increasing magnetic field perpendicular to two-dimensional plane, the Hall resistance ρ_{xy} deviates from classical linear dependence on magnetic flux density B (Eq. (5.15)) and a clear staircase structure emerges. In the IQHE, the heights of the plateaus are exactly

$$\rho_{xy} = \frac{h}{e^2}\frac{1}{n} = \frac{1}{n}\,(\mathrm{R_K}) \approx \frac{2.5812\times 10^4}{n}\,(\Omega), \quad (n = 1, 2, \dots). \tag{10.15}$$

As can be guessed in Fig. 10.4, in the plateau regions simultaneously $\rho_{xx} = 0$, that is, finite current flows without longitudinal voltage. The current here is, like superconductivity, a kind of supercurrent without energy dissipation.

10.2.4 Explanation based on edge mode transport

Comparing the experiment shown in Fig. 10.4 and the localization/delocalization diagram in Fig. 10.3(b), we see that the supercurrent which causes $\rho_{xx} = 0$ flows and ρ_{xy} is quantized when E_F does not exist in the regions of delocalized states. To put this the other way around, ρ_{xy} is in a transient region between quantized plateaus when E_F exists in the retions of delocalization. Namely the quantization and supercurrent take place when two-dimensional electrons are insulating in the bulk.

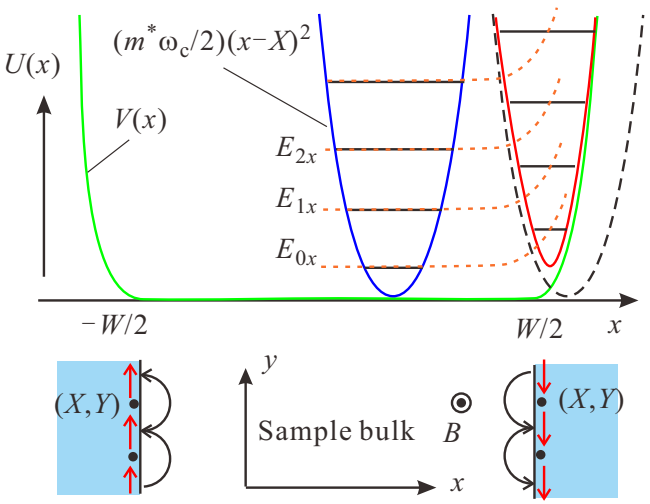

Fig. 10.5 Two-dimensional electrons under strong magnetic field are confined by "gutter-like" potential $V(x)$. The effective potential including the effect of magnetic field is expressed as $U(x)$ (sum of $V(x)$ and magnetic confinement potential). Formation of edge states is indicated by broken lines. The lower panel illustrates classical skipping orbits.

The "edge state model" explains the phenomenon based on edge mode transport. A sample with a finite width as illustrated in Fig. 10.4 inevitably has edge states[*2]. To model that, we consider a two-dimensional electron gas confined in x-direction by a well-like potential $V(x)$ with width W, spreading over y. In this model the current is applied in y-direction (for convenience the coordinate is rotated by $\pi/2$).

$V(x)$ is added to Eq. (10.10) for the wave equation. Figure 10.5 illustrates the situation, in which the gutter-like potential and the harmonic potential by magnetic field co-exist. $V(x) = 0$ deep inside the bulk and ordinary Landau quantization takes place while in the vicinity of edges, $V(x)$ makes the effective harmonic potential narrower, i.e. effective ω_c larger, hence Landau levels go up with approaching the edges. The increase of n-th Landau level begins where X-coordinate of guiding center is in the width of wavefunction $\sqrt{2n+1}l_B/2$ to the edge. In the region of such level increase,

$$\langle v_y \rangle = dE/\hbar dk = -(l_B^2/\hbar)dE/dX \tag{10.16}$$

becomes finite, giving spatial motion to Landau quantized electrons. Such mobile states correspond to classical skipping orbits, which consist of cyclotron motions and collisions to an edge as illustrated in the lower panel of Fig. 10.5. They are called **edge states**. In the edge states the direction of electron motion is determined by the sign of magnetic field.

Normalizing the edge mode wavefunction in the length L_y along y, the current brought by the mode is $j = (e/L_y)\langle v_y \rangle$. A single mode at one-side edge is occupied up to the electrochemical potential μ. We take a base energy E_0 lower than μ and higher than the bulk Landau level with the same Landau index as the edge mode. The current brought by the electrons occupying the states from E_0 to μ in this edge state is obtained from (10.13) and (10.16) as

$$J = \int_{X_0}^{X_\mu} \frac{L_y dX}{2\pi l_B^2} \frac{e}{L_y} \langle v_y \rangle = \frac{e}{h} \int \mathrm{d}X \frac{\mathrm{d}E}{\mathrm{d}X} = \frac{e}{h}(\mu - E_0). \tag{10.17}$$

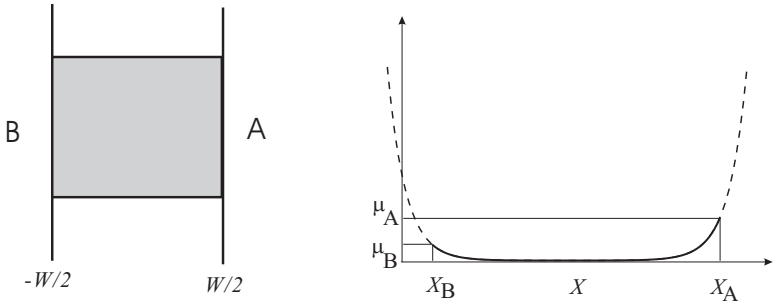

Fig. 10.6 Schematic drawing of a Landau level with edge modes. Finite net current is flowing perpendicular to the figure (y-direction) and consequently finite gradient in x-direction is given (exaggerated).

[*2] There is no edge state along the current if the two edges are connected. Such a structure in a plane is called "Corbino disk."

When $E_{\rm F}$ is in regions of localization, in equilibrium the chemical potential is uniform over the sample and the edges opposite to each other have counter-flowing currents with the same amount, the bulk states are localized and the net current is zero (circular equilibrium current is flowing at the edge). Now we apply the boundary condition that the net current J_y flows along y. As in Fig. 10.6, J_y is the difference between currents $J_{\rm A}$ and $J_{\rm B}$ at edges A and B respectively. Hence from Eq. (10.17), there should be a difference between $\mu_{\rm A}$ and $\mu_{\rm B}$, which leads to the Hall voltage. Then

$$\sigma_{xy} = \frac{J_y}{V_x} = \frac{e(J_{\rm A} - J_{\rm B})}{\mu_{\rm A} - \mu_{\rm B}} = \frac{e^2}{h}. \tag{10.18}$$

This is the conductivity for single Landau level, and for ν levels σ_{xy} is ν times of this value, thus the IQHE is explained.

The above derivation is the same as that of the Landauer formula other than crossing of x and y. The quantization is not so pricise for QPC conductance while surprizingly high precision is achieved for IQHD because of the chirality and the geometrical effect in the edge modes. In the case of QPC, conductance channels with opposite direction are spatially overlapped and backscattering of electrons can easily occurs. On the other hand in the case of IQHE, there is a macroscopic spatial distance between counter-flowing edge states and the probability of backscattering is astronomically low, and the transmission coefficient is exactly one. Therefore, the quantization of IQHE should be inaccurate if the sample width is narrowed and scattering between the edge states is likely to occur, which has been confirmed by experiments. In the above simple model, we ignore the Hall electric field inside the sample. dE/dX caused by the Hall electric field leads to finite bulk current though they cancel each other, does not contribute to J_y and the above discussion still holds.

10.3 Explanation based on topological invariant

We continue theoretica explanation for IQHE. In this section, we need to introduce several new concepts. Below we continue along Ref. [4].

10.3.1 Bloch electrons in magnetic field

We expand the concept of Bloch electron to two-dimensional electrons in magnetic field. This way of treatment is close to tight-binding model while that in Sec. 10.1 is based on two-dimensional free electron. In a two-dimensional square lattice, we write the translational operator by lattice vector $\boldsymbol{R}$ as $T_{\boldsymbol{R}}$.

$$T_{\boldsymbol{R}} f(\boldsymbol{r}) = f(\boldsymbol{r} + \boldsymbol{R}).$$

By expanding $f(\boldsymbol{r})$ with plane wave $e^{i\boldsymbol{k}\boldsymbol{r}}$, from $T_{\boldsymbol{R}} e^{i\boldsymbol{k}\boldsymbol{r}} = e^{i\boldsymbol{k}(\boldsymbol{r}+\boldsymbol{R})} = e^{i\boldsymbol{k}\boldsymbol{R}} e^{i\boldsymbol{k}\boldsymbol{r}}$, $T_{\boldsymbol{R}}$ is written as

$$T_{\boldsymbol{R}} = \exp\left(\frac{i}{\hbar}\boldsymbol{R}\cdot\boldsymbol{p}\right). \tag{10.19}$$

$T_{\boldsymbol{R}}$ commutes with $\mathscr{H}_0$ (lattice Hamiltonian for zero magnetic field) and the Bloch states are defined as the eigenstates that diagonalize the two operators simultaneously.

We then proceed to treat a system under a uniform magnetic field.

$$\mathscr{H} = \frac{1}{2m}(\boldsymbol{p} + e\boldsymbol{A})^2 + V(\boldsymbol{r}). \tag{10.20}$$

The lattice potential $V(\boldsymbol{r})$ is invariant for the operation of $T_{\boldsymbol{R}}$ though the vector potential $\boldsymbol{A}$ is not. Generally

$$\boldsymbol{A}(\boldsymbol{r}) = \boldsymbol{A}(\boldsymbol{r} + \boldsymbol{R}) + \boldsymbol{\nabla} g(\boldsymbol{r}).$$

The loss of translational symmetry due to the cyclotron motion, which does not conserve momentum. Now we consider modification of the translation operator. We define **magnetic translation operator** by replacing $\boldsymbol{p}$ with $\boldsymbol{p} + e\boldsymbol{A}$ in Eq. (10.19). Under symmetric gage $\boldsymbol{A} = \boldsymbol{B} \times \boldsymbol{r}/2$, the magnetic translation operator $T_{B\boldsymbol{R}}$ is given by

$$T_{B\boldsymbol{R}} \equiv \exp\left\{\frac{i}{\hbar}\boldsymbol{R}\cdot\left[\boldsymbol{p} + \frac{e}{2}(\boldsymbol{r}\times\boldsymbol{B})\right]\right\} = T_{\boldsymbol{R}}\exp\left[\frac{ie}{\hbar}(\boldsymbol{B}\times\boldsymbol{R})\cdot\frac{\boldsymbol{r}}{2}\right]. \tag{10.21}$$

$T_{B\boldsymbol{R}}$ commutes with $\mathscr{H}$, and there exists a basis which diagonalizes the two operators simultaneously. Care should be taken that the magnetic translational operators do not commute each other generally just like the guiding center coordinates of Landau levels do not. The commutation relation can be represented as a phase factor in

$$T_{B\boldsymbol{R}a}T_{B\boldsymbol{R}b} = \exp(2\pi i\phi)T_{B\boldsymbol{R}b}T_{B\boldsymbol{R}a}, \quad \phi = \frac{eB}{h}ab, \tag{10.22}$$

where a and b are the lengths of unit vectors. Hence ϕ is the magnetic flux piercing a unit cell in the unit of flux quantum h/e. When ϕ is a rational number p/q, commutable set of magnetic translational opertors can be prepared as a lattice limits translational vectors into discrete lattice vectors. To have simpler view, we consider a **magnetic unit cell**, which is defined from magnetic unit vectors $q\boldsymbol{a}$, $\boldsymbol{b}$ corresponding to original unit vectors $\boldsymbol{a}$, $\boldsymbol{b}$. A magnetic lattice vector $\boldsymbol{R}'$ is expressed as

$$\boldsymbol{R}' = n(q\boldsymbol{a}) + m\boldsymbol{b}. \tag{10.23}$$

Then the flux piercing the magnetic unit cell is p (integer) times a flux quantum and the magnetic translational operators $T_{B\boldsymbol{R}'}$ commute each other.

Now we take ψ as a common eigenstate of $\mathscr{H}$ and $T_{B\boldsymbol{R}'}$. Let T_{qa} and T_b (we do not write $B\boldsymbol{R}'$ for simplicity) be elements of the set of $T_{B\boldsymbol{R}'}$, then the eigenvalues are written as

$$T_{qa}\psi = e^{ik_1qa}\psi, \tag{10.24a}$$

$$T_b\psi = e^{ik_2b}\psi, \tag{10.24b}$$

where k_1, k_2 are generalized crystal momenta. In reduced zone representation, k_1, k_2 can be limited in the first **magnetic Brillouin zone** $0 \le k_1 < 2\pi/qa$, $0 \le k_2 < 2\pi/b$. The magnetic eigenstates is written in the Bloch form

$$\psi_{n\boldsymbol{k}}(\boldsymbol{r}) = e^{i\boldsymbol{k}\boldsymbol{r}}u_{n\boldsymbol{k}}(\boldsymbol{r}), \tag{10.25}$$

where n is a band index, $\boldsymbol{k}$ is a generalized momentum. The conditions for $u_{n\boldsymbol{k}}(\boldsymbol{r})$ are as follows.

$$u_{n\boldsymbol{k}}(x+qa, y) = \exp\left(i\frac{\pi py}{b}\right)u_{n\boldsymbol{k}}(x,y), \tag{10.26a}$$

$$u_{n\boldsymbol{k}}(x, y+b) = \exp\left(-i\frac{\pi px}{qa}\right)u_{n\boldsymbol{k}}(x,y). \tag{10.26b}$$

Then if we write $u_{n\boldsymbol{k}}(\boldsymbol{r})$ in the amplitude-phase factor form as $u_{n\boldsymbol{k}}(\boldsymbol{r}) = |u_{n\boldsymbol{k}(\boldsymbol{r})}|\exp[i\theta_{\boldsymbol{k}}(\boldsymbol{r})]$,

$$p\ \text{(integer)} = -\frac{1}{2\pi}\oint d\boldsymbol{l}\cdot\frac{\partial\theta_{\boldsymbol{k}}(\boldsymbol{r})}{\partial\boldsymbol{l}}, \tag{10.27}$$

where the integral route is taken counter clock direction along the edge of magnetic unit cell.

10.3.2 Hall conductivity from linear response theory

In the k·p perturbation for the band calculation, by renormalizing the plane wave part of wavefunction into the Hamiltonian we obtain the equation for the lattice periodic part $u_{n\boldsymbol{k}}(\boldsymbol{r})$. We can go the same way for the tight-binding model in strong magnetic field. Operation of the Hamiltonian in (10.20) on the magnetic Bloch function in (10.25) can be calculated from $\boldsymbol{p}e^{i\boldsymbol{k}\boldsymbol{r}} = e^{i\boldsymbol{k}\boldsymbol{r}}(\hbar\boldsymbol{k} + \boldsymbol{p})$ as

$$(\boldsymbol{p} + e\boldsymbol{A})^2e^{i\boldsymbol{k}\boldsymbol{r}}u_{n\boldsymbol{k}}(\boldsymbol{r}) = e^{i\boldsymbol{k}\boldsymbol{r}}(\hbar\boldsymbol{k} + \boldsymbol{p} + e\boldsymbol{A})^2u_{n\boldsymbol{k}}(\boldsymbol{r}).$$

We can rewrite the Schrödinger equation as

$$\mathscr{H}_{\boldsymbol{k}} u_{n\boldsymbol{k}}(\boldsymbol{r}) = E_{n\boldsymbol{k}} u_{n\boldsymbol{k}}(\boldsymbol{r}), \quad \mathscr{H}_{\boldsymbol{k}} = \frac{1}{2m}(-i\hbar\boldsymbol{\nabla} + \hbar\boldsymbol{k} + e\boldsymbol{A})^2 + V(\boldsymbol{r}). \tag{10.28}$$

Now we utilize Kubo formula for Hall conductivity in (9B.3). We take the basis as magnetic Bloch funtions and state indices are taken as $(n, \boldsymbol{k})$. Velocity operator $\boldsymbol{v}$ can be written as $\boldsymbol{v} = (-i\hbar\boldsymbol{\nabla} + e\boldsymbol{A})/m$, and for the integration in the numerator we write the matrix element of the operator by using braket representation $u_{n\boldsymbol{k}}(\boldsymbol{r}) \to |n, \boldsymbol{k}\rangle$ as

$$\langle n, \boldsymbol{k}|\boldsymbol{v}|m, \boldsymbol{k}'\rangle = \delta_{\boldsymbol{k}\boldsymbol{k}'} \int_0^{qa} dx \int_0^b dy u^*_{n\boldsymbol{k}} \boldsymbol{v} u_{m\boldsymbol{k}'} \equiv \delta_{\boldsymbol{k}\boldsymbol{k}'} \langle n|m\rangle. \tag{10.29}$$

From the periodicity in $\boldsymbol{k}$ space, the integration just on the magnetic unit cell is enough. The normalization should be

$$\int_0^{qa} dx \int_0^b dy |u_{n\boldsymbol{k}}(\boldsymbol{r})|^2 = 1.$$

By using $\boldsymbol{k}$-dependent Hamiltonian in (10.28), we can write down the matrix elements as

$$\langle n|v_x|m\rangle = \frac{1}{\hbar}\left\langle n \left| \frac{\partial \mathscr{H}_{\boldsymbol{k}}}{\partial k_x} \right| m \right\rangle, \tag{10.30a}$$

$$\langle n|v_y|m\rangle = \frac{1}{\hbar}\left\langle n \left| \frac{\partial \mathscr{H}_{\boldsymbol{k}}}{\partial k_y} \right| m \right\rangle, \tag{10.30b}$$

where $\boldsymbol{k} = (k_x, k_y)$. These are further calculated as

$$\left\langle n \left| \frac{\partial \mathscr{H}_{\boldsymbol{k}}}{\partial k_j} \right| m \right\rangle = (E_m - E_n)\left\langle n \left| \frac{\partial u_m}{\partial k_j} \right\rangle = -(E_m - E_n)\left\langle \frac{\partial u_n}{\partial k_j} \right| m \right\rangle, \quad j = x, y. \tag{10.31}$$

Substtuting the above to the Kubo formula (9B.3) to obtain

$$\begin{aligned}
\sigma_{xy} &= -i\frac{e^2}{\hbar}\sum_{\boldsymbol{k}}\sum_n f(E_{n\boldsymbol{k}}) \sum_{m(\neq n)} \left[\frac{\langle n\boldsymbol{k}|\partial\mathscr{H}_{\boldsymbol{k}}/\partial k_x|m\boldsymbol{k}\rangle\langle m\boldsymbol{k}|\partial\mathscr{H}_{\boldsymbol{k}}/\partial k_y|n\boldsymbol{k}\rangle}{(E_{n\boldsymbol{k}} - E_{m\boldsymbol{k}})^2} - \text{c.c.} \right] \\
&= -i\frac{e^2}{\hbar}\sum_{\boldsymbol{k}}\sum_n f(E_{n\boldsymbol{k}}) \sum_{m(\neq n)} \left[\left\langle \frac{\partial u_n}{\partial k_x} \right| m \right\rangle \left\langle m \left| \frac{\partial u_n}{\partial k_y} \right\rangle - \left\langle \frac{\partial u_n}{\partial k_y} \right| m \right\rangle \left\langle m \left| \frac{\partial u_n}{\partial k_x} \right\rangle \right] \\
&= \frac{e^2}{h}\frac{2\pi}{i}\sum_{\boldsymbol{k}}\sum_n f(E_{n\boldsymbol{k}}) \left[\left\langle \frac{\partial u_n}{\partial k_x} \right| \frac{\partial u_n}{\partial k_y} \right\rangle - \left\langle \frac{\partial u_n}{\partial k_y} \right| \frac{\partial u_n}{\partial k_x} \right\rangle \Big].
\end{aligned} \tag{10.32}$$

Now we define a vector field $\boldsymbol{A}_{n\boldsymbol{k}}$ with

$$\boldsymbol{A}_{n\boldsymbol{k}} = \int d^2\boldsymbol{r} u^*_{n\boldsymbol{k}} \boldsymbol{\nabla}_{\boldsymbol{k}} u_{n\boldsymbol{k}} = \langle u_{n\boldsymbol{k}}|\boldsymbol{\nabla}_{\boldsymbol{k}}|u_{n\boldsymbol{k}}\rangle. \tag{10.33}$$

We assume $T = 0$ and that E_{F} is in the localized region. Writing the summation on $\boldsymbol{k}$ as the form of integration, σ_{xy} is given by

$$\sigma_{xy} = \frac{e^2}{h}\frac{1}{2\pi i}\sum_{E_n < E_{\mathrm{F}}} \int_{\mathrm{MBZ}} d^2k [\boldsymbol{\nabla}_{\boldsymbol{k}} \times \boldsymbol{A}_{n\boldsymbol{k}}]_{k_z} = \frac{e^2}{h}\frac{1}{2\pi i}\sum_{E_n < E_{\mathrm{F}}} \int_{\mathrm{MBZ}} d^2k [\mathrm{rot}_{\boldsymbol{k}} \boldsymbol{A}_{n\boldsymbol{k}}]_{k_z}. \tag{10.34}$$

The integration is over the magnetic Brillouin zone.

Because at the edges of a magnetic Brillouin zone, $k_x = 0$ and $k_x = 2\pi/qa$, $k_y = 0$ and $k_y = 2\pi/b$ are the same points, topologically the zone is two-dimensional torus $T^2 = S^1 \times S^1$. When $\boldsymbol{A}_{n\boldsymbol{k}}$ is single-valued on this torus, σ_{xy} calculated from (10.34) is zero as known from the Stokes theorem. That is, for $\sigma_{xy} \neq 0$, $\boldsymbol{A}_{n\boldsymbol{k}}$ should have non-trivial topology. Here it is important that the magnetic Brillouin zone is a torus, which cannot be squeezed continuously to single point. If such squeezing is possible, $\boldsymbol{A}_{n\boldsymbol{k}}$ defined on the manifold cannot have non-trivial topology.

To see the topology of $\boldsymbol{A}_{n\boldsymbol{k}}$, we consider **local gauge transformation**. A solution of Schrödinger equation (10.28) $u_{\boldsymbol{k}}(\boldsymbol{r})$ can be transformed with an arbitrary continuous function $f(\boldsymbol{k})$ to another solution

$$u'_{\boldsymbol{k}}(\boldsymbol{r}) = \exp[if(\boldsymbol{k})]u_{\boldsymbol{k}}(\boldsymbol{r}). \tag{10.35}$$

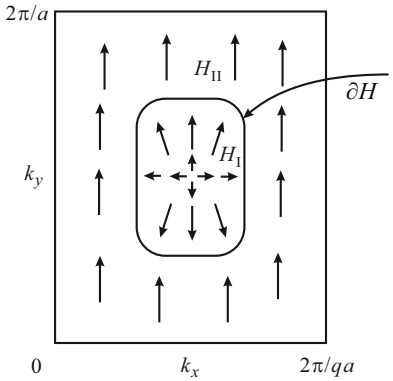

Fig. 10.7 Illustration of phase of wavefunction when it has zero in the magnetic Brillouin zone.

u and u' are physically the same. From the definition in Eq. (10.33), this transformation corresponds to

$$\boldsymbol{A}'_{n\boldsymbol{k}} = \boldsymbol{A}_{n\boldsymbol{k}} + i\boldsymbol{\nabla}_{\boldsymbol{k}} f(\boldsymbol{k}). \tag{10.36}$$

To eliminate the above uncertainty originated from the gauge undertainty, we assume fixing the phase of $u_{n\boldsymbol{k}}(\boldsymbol{r})$ at one point. With this, though, we cannot fix the entire phase over the whole magnetic Brillouin zone. We assume $u_{n\boldsymbol{k}}(\boldsymbol{r})$ is zero at a point $\boldsymbol{k}_0$. As shown in Fig. 10.7, the magnetic Brillouin zone is devided into retion $H_{\rm I}$ that contains $\boldsymbol{k}_0$ and residual region $H_{\rm II}$. If $H_{\rm I}$ contains a zero, the phase must "rotate" around the zero as in the figure. On the other hand $H_{\rm II}$ should be connected at the edges as a torus and the wavefunction should have different structure in phase. Hence we need to take different gauges in the two regions.

For simplicity we consider the contribution of band n only and n can be omitted. The integrals in (10.34) are, by applying Stokes' theorem to the two regions, given by

$$I = \frac{1}{2\pi i}\left[\int_{\rm I} d^2k[{\rm rot}\boldsymbol{A}]_{k_z} + \int_{\rm II} d^2k[{\rm rot}\boldsymbol{A}]_{k_z}\right] = \oint_{\partial H} (\boldsymbol{A}^{\rm II} - \boldsymbol{A}^{\rm I})\cdot\frac{d\boldsymbol{k}}{2\pi i}. \tag{10.37}$$

The integral over circumference of region II cancels out due to the torus boundary condition (equivalent to "back and forth" integration over a single line). On the boundary ∂H, with gauge transformation the relation of the wavefunction is expressed as

$$u^{\rm I}_{\boldsymbol{k}} = u^{\rm II}_{\boldsymbol{k}} e^{i\theta(\boldsymbol{k})}. \tag{10.38}$$

From the definition (10.33), the integral should be

$$I = \oint_{\partial H}\left[\langle u^{\rm II}_{\boldsymbol{k}}|\boldsymbol{\nabla}_{\boldsymbol{k}}|u^{\rm II}_{\boldsymbol{k}}\rangle + (i\boldsymbol{\nabla}_{\boldsymbol{k}}\theta)\langle u^{\rm II}_{\boldsymbol{k}}|u^{\rm II}_{\boldsymbol{k}}\rangle - \langle u^{\rm II}_{\boldsymbol{k}}|\boldsymbol{\nabla}_{\boldsymbol{k}}|u^{\rm II}_{\boldsymbol{k}}\rangle\right]\cdot\frac{d\boldsymbol{k}}{2\pi i} = \frac{\Delta_{\partial H}\theta}{2\pi}. \tag{10.39}$$

The phase evolution over single circulation on the boundary $\Delta_{\partial H}\theta$ should be an integer times 2π and I is limited to an integer. Let $\nu_{\rm C}$ be that integer. And let n_B be the number of bands lower or at the same level as $E_{\rm F}$, we find

$$\sigma_{xy} = n_B\nu_{\rm C}\frac{e^2}{h}, \tag{10.40}$$

which tells that the Hall conductance should be an integer times e^2/h. Equation (10.40) is called **Thouless-Kohmoto-Nightingale-Nijs** (**TKNN**) formula[5]. $\nu_{\rm C}$ is called **Chern number** and known to be 1 for the Landau bands. The above gives the same result as Eq. (10.18).

Chern number is the number of anomalies in the phase of wavefunction, equivalently the number of zeros. It is a kind of **topological invariant**. The origin of Chern number is in the topological property of energy bands. In order to turn a torus into a sphere, we should once tear up the surface around the hole then sew the surfaces together and finally erase the hole. Similarly to change the band structure into the one with different topology (Chern number), we need to crush the band gap once. For this reason, the Hall conductance found in TKNN formula is stable and precise regardless of the variety of sample properties.

Here $\boldsymbol{A}_{\boldsymbol{k}}$ is a Berry connection, ${\rm rot}\boldsymbol{A}_{\boldsymbol{k}}$ is a Berry curvature in Appendix 9A. We will revisit them in the section of topological insulator.

10.3.3 Laughlin's gedankenexperiment

Robert Laughlin considered a sample in which a 2DEG is rolled into a cylinder with a radius of R and a circular electrode is attached to the end of the cylinder (Fig. 10.8)[6]. The magnetic field is emitted outward from the core of the cylinder and is applied perpendicularly to the 2DEG. x and y axes are taken as in the figure. There is no edge because the current is applied along x and the sample is closed along y. Further, a thin, long solenoid is placed at the core and an applied current creates a magnetic flux Φ through it. The flux does not touch the 2DEG directly but gives an AB phase on orbits going around the cylinder. The vector potential for the perpendicular magnetic field and that for the field by the solenoid are in Ladau gauge

$$\boldsymbol{A} = (0, Bx), \quad \boldsymbol{A}_\Phi = \left(0, -\frac{\Phi}{2\pi R}\right). \tag{10.41}$$

We write down the wavefunction in the form of Eq. (10.12). Because the system is circular in y-directoin, the wavefunction should go around the circle.

The current in y-direction is

$$j_y = \frac{1}{L_x}\frac{\partial \mathscr{E}_t}{\partial \Phi}. \tag{10.42}$$

$\mathscr{E}_t$ is the total energy on the cylinder per the normalization length L_x [*3]. The vector potential in Landau gauge is $\boldsymbol{a} = (0, Bx - \Phi/L_y, 0)$. We take the unperturbed Hamiltonian $\mathscr{H}_0$ as the one of 2DEG under magnetic field. Then the effect of solenoid flux is taken into account by the transformation

$$k_y \to k_y - \frac{2\pi}{L_y}\frac{\Phi}{\phi_0}, \quad \left(\phi_0 \equiv \frac{h}{e}\right) \tag{10.43}$$

in the Hamiltonian. This transformation corresponds to the variation in X-coordinate of the guiding center as

$$X \to X + \left(\frac{\Phi}{\phi_0}\right)\frac{L_x}{N_\phi}. \tag{10.44}$$

Then the variation in penetration magnetic flux $\Phi \to \Phi + \Delta\Phi$ appears as that in X $\Delta X = (L_x/N_\phi)\Delta\Phi/\phi_0$. If $\Delta\Phi$ is an integer (q) times ϕ_0, then $\Delta X = qL_x/N_\phi = 2q\pi l_B^2/L_y$, which is q times the distance in x between the eigenstates. Namely the states shift to q-th next eigenstates and the variation in Φ is absorbed into the phase of wavefunction. When

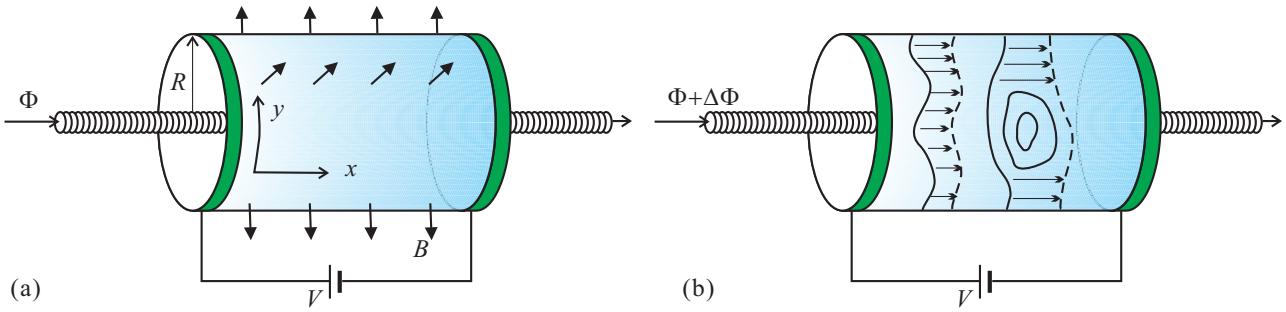

Fig. 10.8 (a) Rolled up two-dimensional system used in Laughlin's gedankenexperiment. The magnetic field B is emitted outward from the core of the cylinder and is applied perpendicularly to the 2DEG. A thin, long solenoid is running at the core of the cylinder giving an AB phase. The electric field is applied in x-direction. (b) Schematic drawing of the variation in wavefunction when the flux by the solenoid is increased from Φ to $\Delta\Phi$.

[*3] Here we prove the equation simply as follows. Let $\mathscr{L}$ be the inductance of the cylinder. A state with current J has the magnetic energy $\mathscr{E}_H = \mathscr{L}J^2/2 = \Phi^2/2\mathscr{L}$, which means $\partial\mathscr{E}_H/\partial\Phi = \Phi/\mathscr{L} = J$. Let L_x be the normalization length. From $J = L_x j_y$ we reach the equation.

N Landau levels are completely occupied, that is $\nu = N$, and there is an electric field of E in x, the variation of $\Delta\Phi = \phi_0$ causes a variation in the energy of $\Delta\mathscr{E} = -eE\Delta X N_e$ ($N_e = \nu N_\phi = N N_\phi$).

Here we assume as follows. In the quantum Hall state, the current does not depend on the boundary condition in y-direction. In other words the current does not depend on the absolute value of Φ. Then we replace the derivative in (10.42) with the finite differece to find

$$j_y = \frac{1}{L_x}\frac{\partial \mathscr{E}_t}{\partial \Phi} = \frac{1}{L_x}\frac{\Delta \mathscr{E}_t}{\Delta \Phi} = \frac{1}{L_x}\left(-eE\frac{L_x}{N_\phi}\right)\frac{N_e}{\phi_0} = N\frac{e^2}{h}E. \tag{10.45}$$

That is the Hall conductance $\sigma_{xy} = j_y/E_x$ is quantized as an integer times e^2/h. Because e^2/h is the conductance for single band, this is an indirect proof that the Chern number of single Landau level is one.

Appendix 9A: The Berry phase

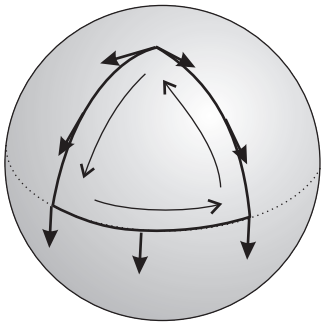

A common classic example of the Berry phase is the parallel displacement of a vector on a sphere as shown on the left. When the vector is translated in three-dimensional space on an appropriate trajectory and return to the original point, the vector does not change. However if we apply a constraint that the vector should be in-plane during the "parallel displacement" (or the vector should be in the tangent plane of the sphere), then as in the left figure, the direction of the vector generally changes when the vector origin comes back to the starting point. The angle between the starting vector and the returning vector corresponds to the Berry phase.

Let α be the angle of variation in the direction of the vector, C be the tranjectory, then α can be expressed as a line integral on C of a vector $\boldsymbol{A}$. This $\boldsymbol{A}$ is called **Berry connection** (Berry connection depends on the constraints on the vector movement). From Stokes' theorem α can also be written as the integration over an area S rimmed by C as

$$\alpha = \oint_C \boldsymbol{A}\cdot d\boldsymbol{s} = \int_S \mathrm{rot}\boldsymbol{A}\cdot d\boldsymbol{\sigma},$$

where $\mathrm{rot}\boldsymbol{A}$ is called **Berry curvature**.

Let us go to quantum mechanics. We consider a time-dependent Hamiltonian $H(t)$ and write the eigenvalue equation as

$$H(t)|n(t)\rangle = E_n(t)|n(t)\rangle. \tag{9A.1}$$

Taking time-derivatibe and operating the eigenfunction $\langle k|$ from left we get

$$\langle k(t)|\partial|n(t)\rangle/\partial t \equiv \langle k(t)|\dot{n}(t)\rangle = \frac{1}{E_n(t)-E_k(t)}\left\langle k(t)\left|\frac{\partial H}{\partial t}\right|n(t)\right\rangle. \tag{9A.2}$$

$$\therefore \langle \dot{n}|n\rangle + \langle n|\dot{n}\rangle = 0 \quad \therefore \mathrm{Re}(\langle n|\dot{n}\rangle) = 0. \tag{9A.3}$$

Let $\psi(t)$ be a solution of the Schrödinger equation composed of $H(t)$. $\psi(t)$ is expanded by $|n(t)\rangle$ as

$$|\psi(t)\rangle = \sum_n c_n(t)|n(t)\rangle \exp\left(-\frac{i}{\hbar}\int_0^t E'_n(t')dt'\right), \quad (E'_n(t) \equiv E_n(t) - \hbar\eta_n(t), \quad \eta_n(t) = i\langle n|\dot{n}\rangle). \tag{9A.4}$$

Substituting this into the Schrödinger equation we find

$$\sum_n i\hbar\left(\dot{c}_n|n\rangle + c_n|\dot{n}\rangle - \frac{i}{\hbar}E'_n c_n|n\rangle\right)\exp\left[-\frac{i}{\hbar}\int_0^t E'_n(t')dt'\right] = \sum_n c_n H|n\rangle \exp\left[-\frac{i}{\hbar}\int_0^t E'_n(t')dt'\right]. \tag{9A.5}$$

Operating $\langle k|$ from the left, from Eq. (9A.2) we obtain

$$\frac{dc_k}{dt} = \sum_{n\neq k} \frac{\langle k|\partial H/\partial t|n\rangle}{E_k - E_n} \exp\left[\frac{i}{\hbar}\int_0^t (E'_k(t') - E'_n(t'))dt'\right] c_n. \tag{9A.6}$$

We consider variation of $H(t)$ slow enough for the variation of the wavefunction to be adiabatic. We take the starting point of the wavefunction $\psi(0) = |m(0)\rangle$ and the adiabatic change means $|\psi(t)\rangle = |m(t)\rangle$ with no mixing of other eigenstates. Let us express the time evolution of H as that in a set of parameters $\{R_i(t)\}$, which can be written in the vector form $\boldsymbol{R}(t)$. We consider a loop trajectory in $\boldsymbol{R}$-space starting $\boldsymbol{R}(0)$ at $t = 0$ and coming back to $\boldsymbol{R}(0)$ at time T.

$$|\psi(t) = |m(\boldsymbol{R}(t))\rangle \exp\left[-\frac{i}{\hbar}\int_0^t E'_m(t')dt'\right] = |m(\boldsymbol{R}(t))\rangle \exp\left[-\frac{i}{\hbar}\int_0^t E_m(t')dt'\right] e^{i\gamma_m(t)}, \tag{9A.7}$$

$$\text{where} \quad \gamma_m(t) = \int_0^t \eta_m(t')dt' = i\int_0^t \langle m(\boldsymbol{R}(t'))|\dot{m}(\boldsymbol{R}(t'))\rangle dt'. \tag{9A.8}$$

As known from (9A.3), γ_m is a real number. For a loop trajectory, with variable transformation $t \to \boldsymbol{R}$,

$$\gamma_m(T) = i\int_0^T \langle m(\boldsymbol{R}(t))|\nabla_R m(\boldsymbol{R}(t))\rangle \cdot \dot{\boldsymbol{R}}(t)dt = i\oint_C \langle m(\boldsymbol{R}(t))|\nabla_R m(\boldsymbol{R}(t))\rangle \cdot d\boldsymbol{R}(t))\rangle d\boldsymbol{R} = \gamma_m(C). \tag{9A.9}$$

∇_R is the gradient operator in $\boldsymbol{R}$-space. Below we omit the subscript R. The above equation means with a loop variation of Hamiltonian associated with adiabatic transition of the state, **Berry phase** $\gamma_m(C)$ is added to the wavefunction. Further by using Stokes' theorem,

$$\gamma_m(C) = -\mathrm{Im}\oint_c \langle m(\boldsymbol{R})|\nabla m(\boldsymbol{R})\rangle \cdot d\boldsymbol{R} = -\mathrm{Im}\int_S [\nabla \times \langle m(\boldsymbol{R})|\nabla m(\boldsymbol{R})\rangle] \cdot d\boldsymbol{S} \tag{9A.10}$$

is obtained.

Appendix 9B: Kubo formula for Hall conductivity

The bf Kubo formula is the ultimate form of linear response theory developed from the first half to the middle of the 20th century. There are various mathematically equivalent expressions in the Kubo formula, but here we introduce what is called Nakano-Kubo formula. We consider a two-dimensonal electrons under perturbation eEy of electric field E in y-direction. First order perturbed states $|\alpha'\rangle$ are written by unperturbed eigenstates $|\alpha\rangle$ as

$$|\alpha'\rangle = |\alpha\rangle + \sum_{\beta\neq\alpha} \frac{\langle\beta|eEy|\alpha\rangle}{E_\alpha - E_\beta}|\beta\rangle. \tag{9B.1}$$

To consider the Hall conductance we need to sum up the contributions from each $|\alpha'\rangle$ to the current along x-direction. Then the current density in x-direction to the first order of perturbation is written as

$$j_x = \frac{1}{L^2}\sum_\alpha f(E_{\alpha'})\langle\alpha'|\hat{j}_x|\alpha'\rangle = \frac{1}{L^2}\sum_\alpha f(E_\alpha)\sum_{\beta\neq\alpha} \frac{\langle\alpha|(-ev_x)|\beta\rangle\langle\beta|eEy|\alpha\rangle}{E_\alpha - E_\beta} + \text{c.c.}, \tag{9B.2}$$

where $f(E)$ is the Fermi distribution function, L^2 is the area of normalization. Because the perturbation term is odd function, there is no first order energy correcltion, and $E_{\alpha'} = E_\alpha$. From

$$\langle\beta|v_y|\alpha\rangle = \langle\beta|\dot{y}|\alpha\rangle = -\frac{i}{\hbar}\langle\beta|[y,\mathscr{H}]|\alpha\rangle = -\frac{i}{\hbar}(E_\alpha - E_\beta)\langle\beta|y|\alpha\rangle,$$

this $\langle\beta|y|\alpha\rangle$ is substituted into Eq. 9B.2 to obtain

$$\sigma_{xy} = \frac{j_x}{E} = \frac{e^2\hbar}{iL^2}\sum_\alpha f(E_\alpha)\sum_\beta \frac{\langle\alpha|v_x|\beta\rangle\langle\beta|v_y|\alpha\rangle}{(E_\alpha - E_\beta)^2} + \text{c.c.}. \tag{9B.3}$$

Appendix 9C: Fractional quantum Hall effects

In the quantum Hall effect, various novel phenomena and ideas have been found. Among them we have a very short look at the fractional quantum Hall effect.

9C.1 Experiment on fractional quantum Hall effects

Fractional Quantum Hall Effect (FQHE) was found in transport experiment in a high-mobility 2DEG. In IQHE, the Hall conductance plateaus appear at $\sigma_{xy} = nG_q$ (n is an integer) while in FQHE the conductance plateaus appear at

$$\sigma_{xy} = fG_q, \quad f = \frac{m}{n} \ \ (n : \text{odd integer}, \ \ m : \text{integer}). \tag{9C.1}$$

Figure 9C.1 shows a representative mesurement of FQHE. The result contains IQHE though the widths of the plateaus are not prominent and rather the behavior is on the classical line. And at the positions in (9C.1), narrow plateaus are observed. On the other hand, the behavior of ρ_{xx} against the magnetic field is dramatic. Even for narrow plateaus at positions (9C.1), ρ_{xx} goes to zero or becomes very small. Hence fine and steep oscillation is observed. Even in the high magnetic field region where no IQHE is observed (filling factor $\nu < 1$), fine oscillation is observed. In particular an oscillation symmetric to $\nu = 1/2$ is observed.

FQHE is very sensitive to the electron mobility, cannot be observed in low mobility samples. In comparison with IQHE, FQHE is observed at lower temperatures with activation energy of a few K. Generally FQHE is easier to be observed at higher magnetic field.

Before going into the physics, we have a short look at the mutual electron interaction and the localization. As we saw in Sec. 10.2.2, when a 2DEG is under a strong magnetic field, the electrons at the Fermi level are in the edge mode at the equipotential lines of impurity potential. The localized state are the states going around the closed equipotential lines. The electron-electron interaction gives some fluctuation to the impurity potential and there is a possibility to lift the localization.

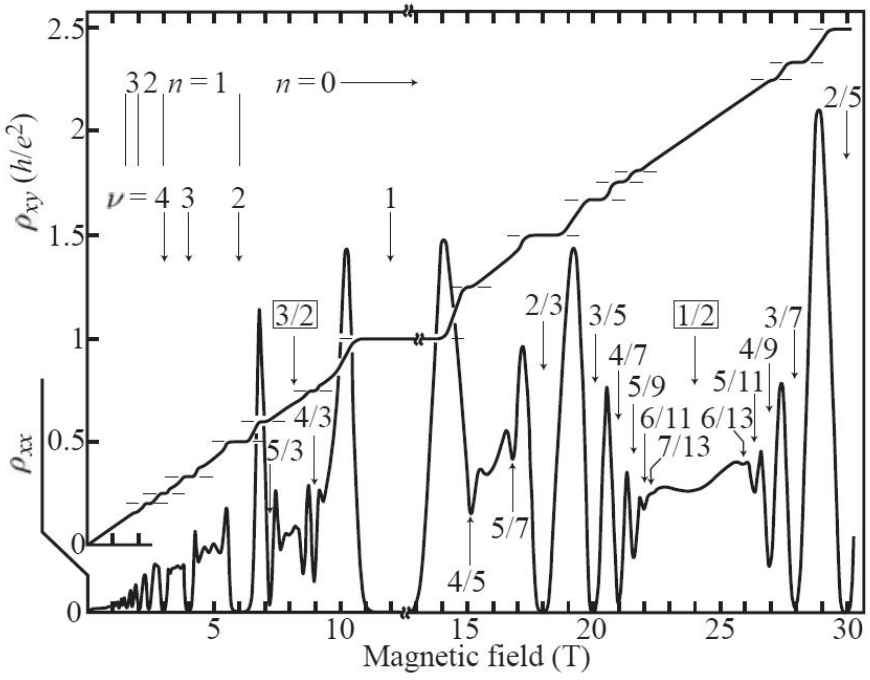

Fig. 9C.1 Representative example of FQHE measurement.

9C.2 Laughlin state

It has been clarified by long-term researches that the electronic states causing FQHE is a kind of electron liquid, in which the electron mutual interaction is dominating the many-body state. The **Laughlin state**, in spite of its simpleness, has been proven to be a good approximation to such electron liquids. This is a big event in many-body physics since the BCS theory.

We again consider a two-dimensional electron system on xy plane in the magnetic field of flux density B. Here for convenience we take the symmetric gauge $\boldsymbol{A} = (-By/2, Bx/2)$. xy-plane can be expressed as a complex plane. The spatial length is measured by the magnetic length. That is, a point on the 2DEG plane can be represented as a complex number $z = (x - iy)/l$. The Hamiltonian with the electron-electron interaction is written as

$$\mathscr{H} = \sum_j \left[\frac{1}{2m}(-i\hbar\nabla + e\boldsymbol{A})^2 + V(z) \right] + \sum_{j<k} \frac{e^2}{|z_j - z_k|}. \tag{9C.2}$$

First we make a many-body wavefunction from single-body wavefunctions at the lowest Landau level without potential and the Coulomb interaction. Then the detail of the many-body wavefunction is determined to minimize the electron interaction energy. The wavefunction which diagonalizes $X^2 + Y^2$, thus the angualr momentum is written as

$$\phi(z) = p(z) \exp\left(-\frac{|z|^2}{l^2} \right), \tag{9C.3}$$

where $p(z)$ is a polynomial of z. Let N_e be the number of electrons and the many-body wavefunction can be written as

$$\psi(z_1, \cdots, z_{N_e}) = f(z_1, \cdots, z_{N_e}) \exp\left(-\sum_i \frac{|z_i|^2}{4} \right), \tag{9C.4}$$

where a polynomial f should be anti-symmetric for the exchange in $(1, \cdots, N_e)$ due to the Pauli principle.

The general form of the terms in f is (coefficient)$\times \prod_i z_i^{m_i}$. This mathematical form indicates that in the state this term represents, the i-th electron is occupying the state with angular momentum $m_i\hbar$. Hence the total angular momentum $\hat{M}$ in this term is $\sum_i m_i\hbar$, and $\hat{M}$ commutes with $\mathscr{H}$. Because $\hat{M}$ represents a conserved quantity, it is desirable to take ψ as to diagonalize $\mathscr{H}$ and $\hat{M}$ simultaneously. For that f should be a homogeneous polynomial.

Further, to make the interaction energy smaller, we consider two-body correlation. The distance between two electrons i and j is $|z_i - z_j|$. Then we try a functional form that f is given by a product of functions g that only depend on $z_i - z_j$, that is

$$f(z_i, \cdots, z_{N_e}) = \prod_{i>j} g(z_i - z_j). \tag{9C.5}$$

From the anti-symmetric property of f, $g(z) = z^q$ and q should be an odd number. The above consideration is summarized into

$$\psi_q(z_1, \cdots, z_{N_e}) = \prod_{i>j} (z_i - z_j)^q \exp\left(-\sum_i \frac{|z_i|^2}{4} \right), \tag{9C.6}$$

which is called **Laughlin state**.

It has been clarified that various ground states exist in a two-dimensional electron system under a strong magnetic field due to strong electron-electron correlation. The Laughlin state is proposed to explain FQHE. As we can guess from the functional form, it is composed to electron interaction energy. It is known that it is close to the exact solution in the finite system obtained by using the exact diagonalization.

9C.3 Filling factor of Laughlin states

In the Laughlin state (9C.6), let us consider the polynomial in front of the exponential. The electron coordinate z_i has a maximum power of $M = (N_e - 1)$. This term of maximum power represents the state, in which the electron indexed i has the maximum angular momentum $M\hbar$. The orbit of this state spreads by l on the circle with a radius $\sqrt{2M}l$. The area corresponding to N_e Landau levels is $2\pi l^2 N_e$ and the filling factor of the state represented by the term is

$$\nu = \frac{2\pi l^2 N_e}{\pi \times 2Ml^2} = \frac{N_e}{M} = \frac{N_e}{(N_e - 1)q} \approx \frac{1}{q}. \tag{9C.7}$$

Among many terms in the polynomial, the ones with largest orbital radius are that gives the largest angular momentum to single electron. Hence the filling factor of this term becomes the filling factor of ψ_q itself. In other words, the filling factor determines q of the corresponding Laughlin state.

9C.4 Excited states

Next we consider the excitation from Laughlin state (9C.6). For that we write the state with increased angular momentum by one for each electron as $\prod_i z_i \psi_q$.

$$\prod_i z_i \psi_q = \prod_i z_i \sum A_{m_1,m_2,\cdots} z_1^{m_1} z_2^{m_2} \cdots z_{N_e}^{m_{N_e}} \exp\left(-\sum_j \frac{|z_j|^2}{4}\right) \tag{9C.8}$$

$$= \sum A_{m_1,m_2,\cdots} z_1^{m_1+1} z_2^{m_2+1} \cdots z_{N_e}^{m_{N_e}+1} \exp\left(-\sum_j \frac{|z_j|^2}{4}\right). \tag{9C.9}$$

The operation of taking the product with $\prod_i z_i$ increases the angular momentum of each electron and at the same time introduces a zero at the origin [*4]. Around the zero, the amplitude of the wavefunction is small with the scale of l and the negative charge density decreases, which can be viewed as a positive charge around the zero. This can be treated as a **quasiparticle**.

We first take the product with $\prod_k (z_k - z_0)^q$, which introduces q quasiparticles at a point z_0. Now we put an electron with spatial size of l at z_0. Then the wavefunction is

$$\prod_k (z_k - z_0)^q \prod_{i<j} (z_i - z_j)^q \exp\left(-\sum_l \frac{|z_l|^2}{4} - \frac{|z_0|^2}{4}\right). \tag{9C.10}$$

This is nothing but a uniform Laughlin state with the electron number increased by one. The above operation means q quasiparticles with a positive charge and an electron with the charge $-e$ are canceled out. This indicates we can cosider that the charge of a quasiparticle is e/q.

9C.5 Composite fermion picture

In a Laughlin state ($\nu = 1/q$), the electrons avoid each other and if we keep our eyes on a single electron, it looks as if a single electron is in a uniform magnetic field. In the $\nu = 1$ Landau level, single a quantum flux Φ_0 is going through the area of a single electron. In the case of Laughlin state the number of quantum magnetic flux per an electron is q. Let us consider such an electron as a "particle" with an even number ($2k$) of quantum flux. Such a particle obeys, if one goes back to Laughlin wavefunction, the Fermi statistices, hence they are called **composite fermion** (CF)[8]. The magnetic field such CFs feels is that of $q - 2k$ times quantum flux.

[*4] With $\prod_i (z_i - z_0)$ zero can be introduced any point z_0.

That is, the field of $q - 2k = 1$ can be seen as IQHE state of $n = 1$ for CFs, where n is the filling factor of CFs. Similarly in the case of $1/(q - 2k) = n > 1$, IQHE of CFs appears for integer n. Because they express extended state of CFs, the electron wavefunction is also extended. There, the filling factor ν of the electrons is

$$\nu = \frac{1}{q} = \frac{1}{2k + 1/n} = \frac{n}{2kn + 1}. \tag{9C.11}$$

For $k = 1$, this gives an FQHE series of 2/5, 3/7, 4/9, $\cdots$, which is comparatively easy to be observed. Taking these states as the starting states, we can explain the next generation of FQH states. The above indicates that the FQHE of electron can be interpreted as IQHE of CFs. ρ_{xx} looks symmetric to $\nu = 1/2$ and the oscillation can be interpreted as SdH oscillation of CFs.

References

[1] K. von Klitzing, G. Dorda, and M. Pepper, Phys. Rev. Lett. **45**, 494 (1980).

[2] Z. F. Ezawa, "Quantum Hall Effects: Recent Theoretical and Experimental Developements", (World Scientifric, 2013).

[3] M. Büttiker, Phys. Rev. B **38**, 9375 (1988).

[4] M. Kohmoto, Ann. Phys. **160**, 343 (1985).

[5] D. J. Thouless, M. Kohmoto, M. P. Nightingale, and M. den Nijs, Phys. Rev. Lett. **49**, 405 (1982).

[6] R. B. Laughlin, Phys. Rev. B **23**, 5632 (1981).

[7] D. J. Thouless, "Topological Quantum Number in Nonrelativistic Physics" (World Scientific, 1998).

[8] J. Jain, "Composite Fermions" (Cambridge, 2007).